# SOA-based All-optical Photonic Integrated Deep Neural Network with Stable Output Noise

Bin Shi[(1),(2)], Nicola Calabretta[(1)], Ripalta Stabile[(1),(2)]

[(1)] Eindhoven Hendrik Casimir Institute, Eindhoven University of Technology, 5600 MB Eindhoven, The Netherlands, b.shi1@tue.nl
[(2)] Eindhoven AI Systems Institute, Eindhoven University of Technology, 5600 MB Eindhoven, The Netherlands

**Abstract** *we experimentally emulate the OSNR evolution of the SOA-based integrated all-optical neuron with 7-channel WDM input to single output conversion, resulting in a stable output error <0.1 and providing noise compression. ©2022 The Authors*

## Introduction

Artificial neural networks (ANN), lying on massive parallel computing, show versatile applications in image classification, feature extraction, and nature language processing etc. Neuromorphic photonics is emerging to develop the alternative approach to electronics, aiming to increase computing speed and energy efficiency [1] as well as to process the optical signal directly. Previously we have demonstrated an integrated all-optical neuron (AON) using WDM inputs and shuffle networks, with semiconductor optical amplifiers (SOAs) and arrayed waveguide gratings (AWGs) technologies, employing SOAs on both linear and nonlinear regimes, enabling two order magnitudes higher speed compared to the GPU [2]. However, an accurate model of the neural network including OSNR degradation building up due to cascading linear and non-linear SOAs is pivotal to evaluate the scalability of these kinds of networks.

In this paper, we propose a noise model for the cascaded SOA-based all-optical neural networks (AONNs), based on the analysis of the noise factor of wavelength converter with noisy inputs. The model exploits the noise figure estimation [3,4] and the small-signal method [4,5]. We measured and simulated the OSNR evolution of SOA-based AONN by tuning the optical signal to noise ratio (OSNR) at the neuron input. The proposed noise evolution model is not only beneficial to the analysis of our neural architecture with the WDM input broadcast, but also can be applied to other WDM-based systems for multi-wavelength input single-wavelength output conversion.

## Experimental Setup

Fig.1a illustrates the AONN with WDM connections, with blue circles shows the all-optical neurons. Fig.1b shows the structure of the SOA-based AON, which consists of the weighted addition unit and nonlinear transfer function (NL-TF). Fig. 1b depicts the schematic of the photonic integrated all-optical neuron with pre-amplifier, weight SOA operated in linear regime and the

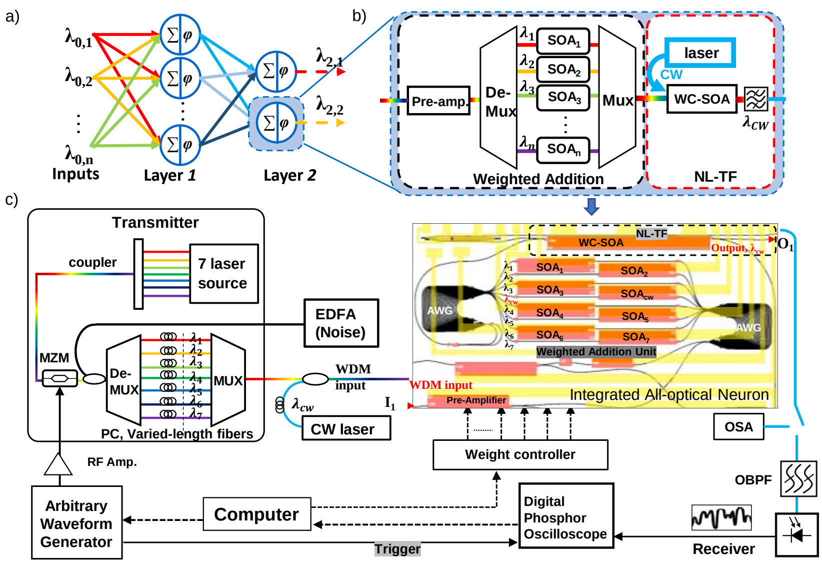

**Fig. 1:** (a) All-optical neural network. (b) SOA-based all-optical neuron. (c)Experimental setup.

power of all the weighted input channels are filtered and summed up via an AWG to re-construct a WDM signal, before being sent to the non-linear function. Fig.1c illustrates the experimental set up. The 7-channel WDM laser sources are operated with wavelengths at 1540.3, 1542.5 1544.8, 1549.5, 1552.1, 1554.5, and 1556.8 nm. After multiplex, the signal is modulated by a PAM modulation on one modulator, driven by an arbitrary waveform generator, with pseudo random bit sequence (PRBS) in 10 Gbit/s. The WDM optical signals are then de-multiplexed and decorrelated using varied lengths of optical fibers before being fed into the neuron, with input power of -17.5 dBm/channel. As shown in Fig. 1b, the red line box shows the NL-TF implemented via a wavelength converter SOA (WC-SOA), with a continuous wave (CW) laser at $\lambda_{cw}$=1546.72 nm, in this case the CW laser is multiplexed to the WDM inputs for better conversion and avoid the poor side-band suppression from on-chip laser [6], which may be improved in the future. The weigh-SOAs are driven with averaged current of 65 mA with multi-current controller to compensate for the path loss and to set different weight factors to the input data. And the current of the WC-SOA is set at 120 mA. The neuron output, after detecting by a linear APD, is recorded by a digital phosphorous oscilloscope (DPO) and post-processed. The AON utilizes a WDM input and provides a single wavelength output. In future this will be part of a full layer of *N* neurons with *M* input wavelengths for all-optical neural network implementation shown in Fig. 1a.

**Simulation method**

we develop a noise model to explain the signal degradation and to evaluate the performance of the all-optical neuron. A back-to-back (B2B) measurement is necessary to determine an equivalent OSNR of the receiving signal at the APD since in-band noise at the converted output channel is not observable on the optical spectrum analyser. The normalized root mean square error (NRMSE) between the measured and expected signal can be estimated as [7]:

$$NRSME \propto \sqrt{N_e}/S \propto \ P_{sp}^2. \qquad (1)$$

where $N_e$ is noise of the photodetector, and $S$ is the span of the optical signal to the receiver and $P_{sp}$ is the optical noise. By setting *S as* constant, the spontaneous-spontaneous beating noise and signal-spontaneous beating noise defines the output error induced from the optical signal processing, with $P_{sp}$ is the spontaneous emission noise to the APD. Using equation (1), we can estimate the equivalent OSNR at the neuron output by measuring the NRMSE for B2B measurement and AON tests.

To estimate the noise from the AON, we need to consider the noise accumulation from the 3 stages of the SOAs: Pre-amplifier, weight SOAs, and WC-SOA, as shown in Fig.1b. The noise from the SOAs at the final converted output can be obtained with calculating the noise figure of the device, which defines the output OSNR.

Considering the SOA chain in Fig.1b, we can obtain the ASE density at the output of the all-optical neuron will be:

$$\rho_{ASE} = \bar{\rho}_{sse} G_1 L_1 G_2 L_2 \eta + \rho_{ASE1} L_1 G_2 L_2 \eta + \rho_{ASE2} L_2 \eta + \rho_{sse,cw} + \rho_{ASE3}(1 + \eta/G_3), \qquad (2)$$

with $\bar{\rho}_{sse}$ is the averaged spontaneous source emission (SSE) for AON inputs and $\rho_{sse,cw}$ is the SSE for CW-laser at WC-SOA input. $\rho_{ASE1}$, $\rho_{ASE2}$, $\rho_{ASE3}$ is the amplified spontaneous emission (ASE) generated by the Pre-amplifier, weight SOAs, and WC-SOA, respectively. $G_1$, $G_2$, and $G_3$ are the gain from pre-amplifier, weight SOA and WC-SOA. The gain and ASE generation is assumed to be the same for all the input channels. $L_1$, $L_2$ are the coupling loss between pre-amplifier and weight SOA, and between weight SOA and WC-SOA. And $\eta$ is the total conversion efficiency from the *M* input channels to single output channel, which is obtained by calculating conversion from individual channel as shown in [8, 9]. Considering the ASE dominates the input and output noise. The noise factor of the AON is:

$$F_{s-sp} = \frac{1}{G'} \frac{\rho_{ASE}}{M \bar{\rho}_{sse}}, \qquad (3)$$

with $G'=P_s/(MP_0)$, and $P_s=G_3P_{0,cw}$ is the converted signal output and $P_0$ is the averaged input power for *M* channels, $P_{0,cw}$ is the input power of the CW-laser at WC-SOA. Seen from equation (2) and (3), $F_{s\text{-}sp}$ is a function of $\bar{\rho}_{sse}$, i.e. different input SSE determines different noise figure. Hence, the output OSNR evolution of the layer connections can be estimated given an input OSNR.

When $F_{s\text{-}sp} \leq 1$, we can derive the condition for arbitrary layer scaling of the all-optical neural network. Equation (3) yields,

$$\bar{\rho}_{sse} \geq \frac{\eta \bar{\rho}_{ASE}/G + G\ \rho_{sse,cw} + \rho_{ASE,cw}}{GP_{cw}/P_0 - \eta}. \qquad (4)$$

As long as $G'M > G_1 L_1 G_2 L_2 \eta$, equation (4) suggests that if input noise is greater to this value, the noise will be compressed, and if $F_{s-sp} = 1$, it is possible the AON can cascade for arbitrary depth.

**Results**

Fig. 2a plots the measured outputs from the 7-channel input to 1 output AON with different input OSNR at 19, 20, and 31 dB, in blue, according to the current set on the EDFA as 300, 150, and 40

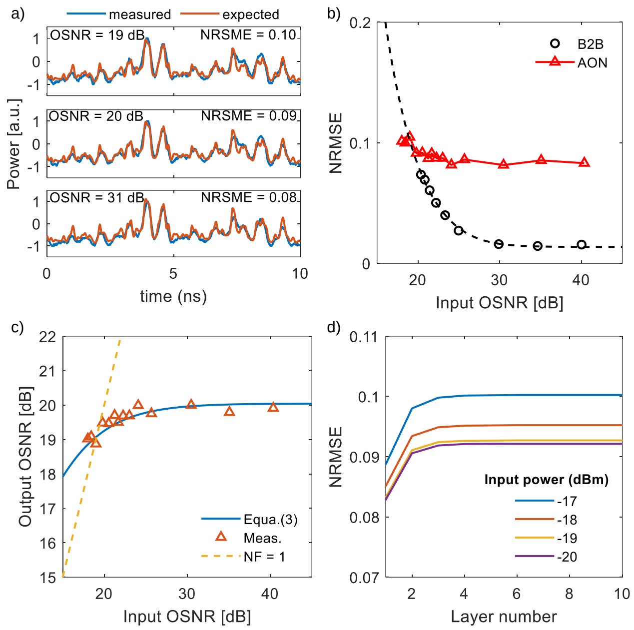


**Fig. 1:** 7-channel input to 1 output AON: (a) Measured (blue) and expected (red) time traces at the output (b) Error vs. the input OSNR for back-to-back (circles) and AON testing (triangles). (c) Output OSNR vs. input OSNR from equation (3) (blue line), measurement (triangles) in (b), and NF = 1(dashed line). (d)Optimization with tuning the input power per channel.

mA, and compared to the expected output from computer, in red, resulting in NRMSE of 0.1, 0.09, and 0.08 with for 7-channel inputs. The error does not significantly change due to limited conversion of noise contribution from the weighting SOA, as shown from equation (3), and with constant the ASE generation from the WC-SOA. The blue circles in Fig.2 plots the error variation for B2B measurements and the squares shows error variations of the 7-channel AON under testing when tuning the input OSNR. The dashed line depicts the fitting with the second order polynomial relation in equation (1). The inverse relation for this B2B measurements (with dashed line) can be used to determine the equivalent OSNR for the measured data.

Figure 2c shows the output OSNR for the 7-channel input AON. The blue line shows the simulation results using the noise factor calculation in equation (3). The red squares present the equivalent OSNR obtained via the relation shown in Fig. 2b. The measured OSNR is agreed with the noise factor calculation. It is worthy to note the dashed line in Fig. 2c shows the I/O OSNR relation for NF = 1, i. e. there is no signal degradation. Apparently, the cross of the blue line and black dashed line shows the noise suppression from the AON, when the input OSNR is lower than 19.1 dB, corresponding to inequation (4), the output OSNR of the AON will be greater than the input OSNR. Hence, when input OSNR = 19.1 dB, the error of the AON will be maximum, since if OSNR< 19.1 dB, the output OSNR will be improved and if OSNR> 19.1 dB the output OSNR will be degraded, and it eventually converges to OSNR = 19.1 dB. Since the NRSME for OSNR = 19.1 dB is 0.10, the error of the 7-channel AON will be <0.10, which paves the way to arbitrary layer connection of all-optical deep neural network. Fig.2d plots the simulated errors when using noise figure defined in equation (3) and shown in Fig. 2c and tuning the input signal power from -17 to -20 dBm/channel. The error of the AONN output with be stabilized in 0.1 after 4 layers, attributing to the noise suppression effect of the multiple input to single output conversion. Furthermore, the model can be used to optimize the input signal power, Fig. 2d suggest the optimized input signal power for the 7-channel neuron is -20 dBm.

## Conclusions

We have demonstrated noise modelling for the SOA-based monolithically integrated all-optical neuron to investigate the error evolution for photonic deep neural network. The result of both experiments and simulations shows a noise compression with multi-wavelength input to single wavelength output conversion, exploiting cross-gain modulation in nonlinear SOA. This paves the way for all-optical deep neural network with stable noise induction for arbitrary depth.

## Acknowledgements

This research work is financially supported by the Netherlands Organization of Scientific Research (NWO) under the Zwaartekracht programma, 'Research Centre for Integrated Nanophotonics'.

## References

[1] B. J. Shastri *et al.*, "Photonics for artificial intelligence and neuromorphic computing," *Nat. Photonics*, vol. 15, no. 2, pp. 102–114, 2021, DOI: 10.1038/s41566-020-00754-y.

[2] B. Shi, N. Calabretta, and R. Stabile, "InP photonic integrated multi-layer neural networks: Architecture and performance analysis," APL Photonics, vol. 7, no. 1, p. 10801, 2022, DOI: 10.1063/5.0066350.

[3] D. M. Baney, et al., "Theory and Measurement Techniques for the Noise Figure of Optical Amplifiers," Opt. Fiber Technol., vol. 6, no. 2, pp. 122–154, 2000, DOI: 10.1006/ofte.2000.0327.

[4] M. J. Connelly, Semiconductor Optical Amplifiers. Boston: Kluwer Academic Publishers, 2002, DOI: 10.1007/b101817.

[5] A. Mecozzi, "Small-signal theory of wavelength converters based on cross-gain modulation in semiconductor optical amplifiers," IEEE Photonics Technol. Lett., vol. 8, no. 11, pp. 1471–1473, Nov. 1996, DOI: 10.1109/68.541553.

[6] B. Shi, K. Prifti, E. Magalhães, N. Calabretta, and R. Stabile, "Lossless Monolithically Integrated Photonic InP Neuron for All-Optical Computation," in Optical Fiber Communication Conference (OFC) 2020 (2020), paper W2A.12, 2020, DOI: 10.1364/ofc.2020.w2a.12.

[7] N. A. Olsson, "Lightwave Systems With Optical Amplifiers," *J. Light. Technol.*, vol. 7, no. 7, pp. 1071–1082, 1989, DOI: 10.1109/50.29634.

[8] K. Obermann, I. Koltchanov, K. Petermann, S. Diez, R. Ludwig, and H. G. Weber, "Noise analysis of frequency converters utilizing semiconductor-laser amplifiers," IEEE J. Quantum Electron., vol. 33, no. 1, pp. 81–88, 1997, DOI: 10.1109/3.554895.

[9] B. Shi, B. Pan, N. Calabretta, and R. Stabile, "Noise analysis of SOA-based All-optical Photonic Deep Neural Network with WDM input," Photonics Switch. Comput. 2021 (2021), paper. Tu3B.4, 2021, DOI: 10.1364/PSC.2021.TU3B.4.